

# Magnetic levitation for hard superconductors

Alexander A. Kordyuk<sup>a)</sup>

*Institute of Metal Physics, 252680 Kiev 142, Ukraine*

(Received 12 June 1997; accepted for publication 23 September 1997)

An approach for calculating the interaction between a hard superconductor and a permanent magnet in the field-cooled case is proposed. The exact solutions were obtained for the point magnetic dipole over a flat ideally hard superconductor. We have shown that such an approach is adaptable to a wide practical range of melt-textured high-temperature superconductors' systems with magnetic levitation. In this case, the energy losses can be calculated from the alternating magnetic field distribution on the superconducting sample surface. © 1998 American Institute of Physics. [S0021-8979(98)01501-1]

The study of systems with levitation has provoked particular interest before<sup>1</sup> and after<sup>2-4</sup> the discovering of high temperature superconductors (HTS) and especially today when melt-textured HTS technology is actively developed.<sup>5,6</sup>

Earlier<sup>7</sup> we described the elastic properties of the point magnetic dipole over a granular HTS sample. We showed that in such a system the granular HTS at 77 K may be considered as a set of small isolated superconducting grains in calculating elastic properties<sup>7</sup> and energy losses.<sup>8</sup> We obtained the information about granular structure and intragrain magnetic flux motion from the investigation of the resonance frequencies<sup>7</sup> and damping coefficients<sup>9</sup> for different modes of the permanent magnet (PM) forced oscillations.

The melt-textured large grain HTS samples that are actively studied now are very different from granular ones in levitation properties. First, they have very strong pinning resulting in the absence of the effect of the PM rise above HTS sample at its cooling. Second, the small isolated grains approximation does not work for large grains.

In this article, the absolutely hard superconductor approach is used. The sense of this approach is to use the surface shielding currents to calculate the magnetic field distribution outside the superconductor and to obtain from it the elastic properties of the PM-HTS system. The magnetic field inside such an ideal superconductor  $\mathbf{B}(\mathbf{r})$  does not change with PM displacements. The feasibility of this approximation is determined by the condition  $d \ll L$ , where  $d$  is the field penetration depth and  $L$  is the character system dimension (first the distance between PM and HTS). With such an approximation, this problem has an exact analytical solution for the case of a magnetic dipole over a flat superconductor in the field cooled (FC) case.

To describe the FC behavior of the PM, the advanced mirror image method was applied. The method is illustrated by Fig. 1. Its distinction from the usual one, which is applied to the type-I superconductors, is in the using of the frozen PM image that creates the same magnetic field distribution outside the HTS as the frozen magnetic flux does. From the uniqueness theorem, the magnetic field distribution in an area with no induced currents is uniquely determined by the normal field component on its boundary. In other words, the distribution of this component determines the PM-HTS inter-

action, and in turn is determined by the PM initial position (FC position). For the PM with initial position  $\mathbf{r}_0 = (x_0, y_0, z_0)$  and magnetic moment  $\boldsymbol{\mu}_0$  (see Fig. 1) that generates the magnetic field  $\mathbf{H}(\mathbf{r} - \mathbf{r}_0, \boldsymbol{\mu}_0)$ , the normal magnetic field component on HTS surface  $\boldsymbol{\rho} = (x, y, 0)$  is equal to the same component of its reverse image with  $\mathbf{r}_0^* = (x_0, y_0, -z_0)$  and  $\boldsymbol{\mu}_0^*$  (the operation \* maps any vector symmetrically about  $\rho$  surface)

$$H_z(\boldsymbol{\rho} - \mathbf{r}_0, \boldsymbol{\mu}_0) = H_z(\boldsymbol{\rho} - \mathbf{r}_0^*, -\boldsymbol{\mu}_0^*). \quad (1)$$

It is required that  $H_z(\boldsymbol{\rho})$  should be unchanged at any PM displacements  $\delta\mathbf{r} = \mathbf{r}_1 - \mathbf{r}_0$  ( $\boldsymbol{\mu}_0 \rightarrow \boldsymbol{\mu}_1$ , Fig. 1) from initial position. To do this, the presence of another image with  $\boldsymbol{\mu}_1^*$  is required. This image moves with PM to  $\mathbf{r}_1^*$  position [ $H_z(\boldsymbol{\rho} - \mathbf{r}_1, \boldsymbol{\mu}_1) + H_z(\boldsymbol{\rho} - \mathbf{r}_1^*, \boldsymbol{\mu}_1^*) = 0$ ]. Thus, the interaction between the PM and shielding current can be described by the interaction of the PM with net field of two images

$$\mathbf{H}_{\text{im}}(\mathbf{r}) = \mathbf{H}(\mathbf{r} - \mathbf{r}_0^*, -\boldsymbol{\mu}_0^*) + \mathbf{H}(\mathbf{r} - \mathbf{r}_1^*, \boldsymbol{\mu}_1^*), \quad (2)$$

and for the field outside and inside the superconductor we can write:

$$\mathbf{B}(\mathbf{r}) = \mathbf{H}(\mathbf{r} - \mathbf{r}_0, \boldsymbol{\mu}_0) + \mathbf{H}_{\text{im}}(\mathbf{r}), \quad (\text{for } z > 0) \quad (3)$$

$$\mathbf{B}(\mathbf{r}) = \mathbf{H}(\mathbf{r} - \mathbf{r}_0, \boldsymbol{\mu}_0) \quad (\text{for } z < 0). \quad (4)$$

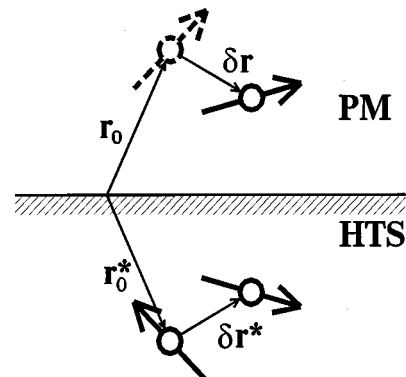


FIG. 1. The advanced mirror image method illustration.

<sup>a)</sup>Electronic mail: kord@imp.kiev.ua

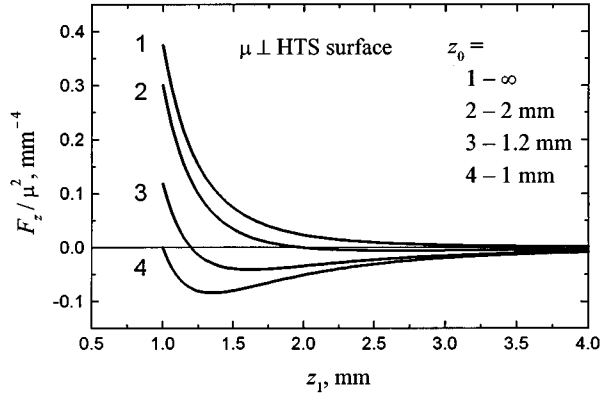


FIG. 2. The levitation force acting on the magnetic dipole with  $\mu_{\parallel z}$  for the different FC positions  $z_0$  vs its distance to the superconducting surface  $z_1$  from Eq. (6).

The above relations are true for any shape of PM where  $\mu$  indicates the direction of volume magnetization. For the case of the point magnetic dipole, the analytical solution can be obtained.

The force acting on the magnetic dipole

$$\mathbf{F}(\mathbf{r}_1) = (\boldsymbol{\mu}_1 \cdot \nabla) \mathbf{H}_{\text{im}} = \left[ -(\boldsymbol{\mu}_1 \cdot \nabla) \nabla \left( \frac{[-\boldsymbol{\mu}_1^*(\mathbf{r} - \mathbf{r}_0^*)]}{|\mathbf{r} - \mathbf{r}_0^*|^3} + \frac{[\boldsymbol{\mu}_1^* + (\mathbf{r} - \mathbf{r}_1^*)]}{|\mathbf{r} - \mathbf{r}_1^*|^3} \right) \right]_{\mathbf{r}=\mathbf{r}_1} \quad (5)$$

can be calculated symbolically for any PM displacement and  $\mu$  direction. For example, for  $\mathbf{r}_1 = (x_0, y_0, z_1)$  and  $\mu_{\parallel z}$

$$F_z(z_1) = 6\mu^2[(2z_1)^{-4} - (z_1 + z_0)^{-4}]. \quad (6)$$

The  $F_z(z_1)$  dependencies for different  $z_0$  are presented in Fig. 2.

The elastic properties of PM-HTS system (oscillation frequencies  $\omega$  and nonlinearities  $\gamma$ ) can be obtained from the expansion of  $\mathbf{F}(\delta\mathbf{r})$  on  $\delta = \delta s/z_0$  (for any mode  $s = x, y, z$ ):

$$F_s(\delta) = -m\mu^2 z_0^{-4} (k_0 \delta + k_1 \delta^2 + k_2 \delta^3) + O(\delta^4), \quad (7)$$

$$\omega = \omega_0 [1 + \gamma(A/z_0)^2], \quad \omega_0 = \mu \sqrt{\frac{k_0}{mz_0^5}}, \quad (8)$$

$$\gamma = \frac{3k_2}{8k_0} - \frac{5}{12} \left( \frac{k_1}{k_0} \right)^2,$$

where  $m$  is PM mass and  $A$  is the PM amplitude. The values of the coefficients  $k$  and  $\gamma$  are presented in the Table I.

The other useful side of this approach is the opportunity to obtain the surface distribution of alternating field  $h(\boldsymbol{\rho})$  and consequently—energy losses. From (3), this field only has a component parallel to the HTS surface  $h(\boldsymbol{\rho}) = h_\rho(\boldsymbol{\rho})$  and is determined by the PM and its moving image (Fig. 1)

$$h(\boldsymbol{\rho}, s) = 2A \left( \frac{\partial H_\rho(r)}{\partial s} \right)_{z=z_0}. \quad (9)$$

For the melt-textured HTS where the energy losses have predominantly hysteretic nature,<sup>5</sup> the feasibility of such ap-

TABLE I. The values of the coefficients  $k$  and  $\gamma$  are calculated from (7) and (8).

$\mu$ direction	Mode $s$	$k_0$	$k_1$	$k_2$	$\gamma$
$\mu_{\parallel z}$	$x=y$	3/8	0	-45/128	-45/128
	$z$	3/4	-45/16	105/16	-165/64
$\mu_{\parallel x}$	$x$	9/32	0	-75/256	-25/64
	$y$	3/32	0	-15/256	-15/64
	$z$	3/8	-45/32	105/32	-165/64

proximation can be determined from the critical state model (the thickness of the layer carrying the critical current  $J_c$  must be well less than PM-HTS distance) and for the above configuration

$$z_0 \gg d = \frac{c}{4\pi} \frac{h(\boldsymbol{\rho}, s)}{J_c}, \quad (10)$$

where  $c$  is speed of light. As this takes place, and as the dimension of the HTS sample is much more than  $d$ , the energy loss per square  $w(\boldsymbol{\rho}) = (c/24\pi^2)h^3(\boldsymbol{\rho})/J_c$ . Then from (9) after integrating the energy loss per PM oscillation period (for  $\mu_{\parallel z}$  case and  $z$  mode for example),

$$W = k \frac{c}{J_c} \frac{\mu^3}{z_0^{10}} A^3, \quad (11)$$

where  $k \approx 0.83$ . From here, the reversed  $Q$  factor of the PM-HTS system<sup>8</sup> is

$$Q^{-1} = \frac{k}{\pi k_0} \frac{c}{J_c} \frac{\mu}{z_0^5} A. \quad (12)$$

The condition (10) is much stronger than is necessary to validate the use of the described approach for melt-textured HTS. Even for  $J_c \sim 10^4$  A/cm<sup>2</sup> and for  $h \sim 100$  Oe, the penetration depth  $d \sim 0.1$  mm. The experimental values of resonance frequencies that we obtained for PM over the single domain HTS sample system ( $m = 0.021$  g,  $\mu = 1.2$  G cm<sup>3</sup>,  $z_0 = 2.5$  mm) are in complete agreement with theoretical ones.<sup>10</sup> If the melt-textured sample has more than one domain, the resonance frequencies and levitation forces are appreciably reduced. Thus the elastic properties of the PM-HTS system can be used to obtain the information about “granularity” of such HTS samples but to determine from this the number of domains per sample the additional investigations are needed. Therewith, the energy losses depend only slightly on such granularity and critical current density in the thin layer  $d$  under HTS surface can be determined from (12) with a high accuracy.

<sup>1</sup>A. F. Hebard, Rev. Sci. Instrum. **44**, 425 (1973).

<sup>2</sup>F. C. Moon, M. M. Yanoviak, and R. Ware, Appl. Phys. Lett. **52**, 1534 (1988).

<sup>3</sup>S. A. Basinger, J. R. Hull, and T. M. Mulcahy, Appl. Phys. Lett. **57**, 2942 (1990).

<sup>4</sup>R. Grosse, J. Jäger, J. Betz, and W. Schoepe, Appl. Phys. Lett. **67**, 2400 (1995).

<sup>5</sup>Z. J. Yang, J. R. Hull, T. M. Mulcahy, and T. D. Rossing, J. Appl. Phys. **78**, 2097 (1995).

<sup>6</sup>T. Sugiura and H. Fujimori, IEEE Trans. Magn. **32**, 1066 (1996).

<sup>7</sup>A. A. Kordyuk and V. V. Nemoshkalenko, Appl. Phys. Lett. **68**, 126 (1996).

<sup>8</sup>A. A. Kordyuk and V. V. Nemoshkalenko, J. Supercond. **9**, 77 (1996).

<sup>9</sup>V. V. Nemoshkalenko and A. A. Kordyuk, Low Temp. Phys. **21**, 791 (1995).

<sup>10</sup>A. A. Kordyuk and V. V. Nemoshkalenko, Phys. Metal. Adv. Technol. (to be published).